Inorganic Chemistry

pubs.acs.org/IC

Article

Unveiling the Structural Behavior under Pressure of Filled $M_{0.5}Co_4Sb_{12}$ (M = K, Sr, La, Ce, and Yb) Thermoelectric Skutterudites

João Elias F. S. Rodrigues,* Javier Gainza, Federico Serrano-Sánchez, Mateus M. Ferrer, Guilherme S. L. Fabris, Julio R. Sambrano, Norbert M. Nemes, José L. Martínez, Catalin Popescu, and José A. Alonso*

Cite This: *Inorg. Chem.* 2021, 60, 7413−7421

Read Online

ACCESS | Metrics & More | Article Recommendations

ABSTRACT: Skutterudite-type compounds based on $\square Co_4Sb_{12}$ pnictide are promising for thermoelectric application due to their good Seebeck values and high carrier mobility. Filling the 8*a* voids (in the cubic space group $Im\bar{3}$) with different elements (alkali, alkali earth, and rare earth) helps to reduce the thermal conductivity and thus increases the thermoelectric performance. A systematic characterization by synchrotron X-ray powder diffraction of different M-filled Co_4Sb_{12} (M = K, Sr, La, Ce, and Yb) skutterudites was carried out under high pressure in the range ∼0−12 GPa. The isothermal equations of state (EOS) were obtained in this pressure range and the Bulk moduli (B_0) were calculated for all the filled skutterudites, yielding unexpected results. A lattice expansion due to the filler elements fails in the description of the Bulk moduli. Topochemical studies of the filler site environment exhibited a slight disturbance and an increased ionic character when the filler is incorporated. The mechanical properties by means of Bulk moduli resulted in being sensitive to the presence of filler atoms inside the skutterudite voids, being affected by the covalent/ionic exchange of the Co−Sb and Sb−Sb bonds.

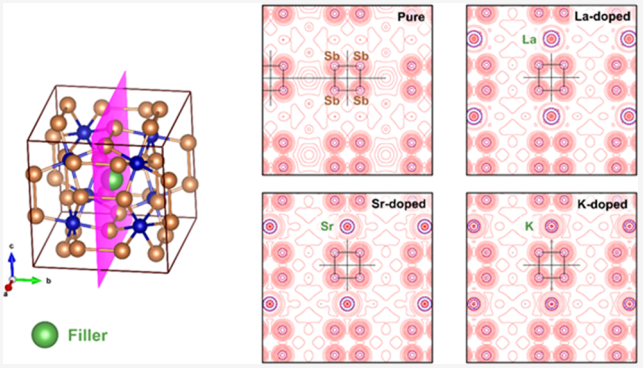

1. INTRODUCTION

In the field of energy conversion technologies, thermoelectric materials have been showing interesting applications in recovering electrical energy from temperature gradients. Well-designed devices can integrate a waste heat recovery system or solid-state-based cooling/heating with no moving parts and long-term stability. Indeed, due to the Peltier effect, these materials can be used in a thermoelectric cooler in several practical applications such as small refrigerators for beverages, CPU cooling, vaccine refrigeration for portable bags, thermal stabilization devices for lasers or CCD detectors, etc. For a better performance, a high efficiency should be achieved through a figure of merit ($zT = S^2\sigma T/\kappa_T$) above 1.[1] This dimensionless parameter has a threefold dependency: the Seebeck coefficient (S), carrier electrical conductivity (σ), and thermal conductivity (κ_T). A good thermoelectric material should balance these three physical quantities in order to provide a reasonable performance for applications.

Among the thermoelectric compounds, the binary skutterudites $\square T_4X_{12}$ (T = Co, Rh, or Ir; X is a pnictogen element) depict interesting Seebeck values and high carrier mobility; however, the thermal conductivity (typically around 10 $Wm^{-1}K^{-1}$) is not so attractive to enhance a value of $zT > 1$, mainly due to the strong covalent bonding of the framework $(TX_3)_4^{3-}$. Such a structure has open cavities (voids: $\square$), which can be filled by guest atoms, thus producing a material with phonon-glass electron-crystal (PGEC) properties.[2,3] As a result, the thermal conductivity might be reduced by an order of magnitude, as the phonon mean free path is decreased due to the presence of fillers. The local bonding of the filler inside the cavities plays a pivotal role for enhancing the zT parameter. Rare-earth elements have been usually a common choice to fill these voids, with plenty of examples reported in the literature.[4−10] Recently, our group demonstrated that the high-pressure synthesis is an effective tool to stabilize lanthanides into the voids of the $\square Co_4Sb_{12}$ skutterudite,[11] as in the case of La,[12] Ce and Yb,[13] and mischmetal,[14] consequently reducing the thermal conductivity (<2−3 $Wm^{-1}K^{-1}$).

Received: March 5, 2021
Published: April 26, 2021

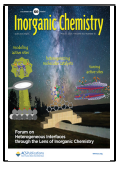

Under the application of an external high-pressure, some interesting features were observed in filled skutterudites, including a metal−insulator transition in $PrFe_4P_{12}$ at 2.4 GPa and an insulator−metal transition in $PrRu_4P_{12}$ at 12 GPa.[15] Another example is the filling fraction in $CoSb_3$ skutterudites, which is enlarged with increasing the applied pressure,[16] and sometimes, the high-pressure synthesis is the only procedure that can be used to introduce a certain filler element.[17,18] $\square Co_4Sb_{12}$ presented self-insertion reactions, in which the transition $\square Co_4Sb_{12} \rightarrow Sb_xCo_4Sb_{12-x}$ takes place under high pressure with no volume discontinuity.[19] The elastic properties of filled skutterudites may unveil details on the local bonding of the fillers inside the voids and, therefore, useful insights into the features of PGEC systems.

Herein, we provide a structural investigation by synchrotron radiation in unfilled $\square Co_4Sb_{12}$ and filled $M_{0.5}Co_4Sb_{12}$ (M = K, Sr, La, Ce, and Yb) skutterudites, previously synthesized under high-pressure conditions (3.5 GPa) and studied also under compression with pressures up to 12 GPa. The isothermal equations of state (EOS) were determined in this pressure range, and the Bulk moduli (B_0) were obtained for all the filled skutterudites. Computational calculations by means of density functional theory were also conducted in order to give light about the filler local environment and involved chemical interactions. We aim to correlate the lattice expansion due to the filler atoms with the Bulk moduli experimentally derived and possible consequences from a local point of view.

2. EXPERIMENTAL SECTION

2.1. High-Pressure Synthesis. Pure Co_4Sb_{12} and filled skutterudites of nominal composition $M_{0.5}Co_4Sb_{12}$ (M = K, Sr, La, Ce, and Yb) were synthesized under high pressure (HP) at moderate temperatures in a piston-cylinder press (Rockland Research Co). Stoichiometric amounts of M, Co, and Sb were mixed and ground in a N_2-filled glove box to avoid surface oxidation. Ternary elements M were taken from metallic powders, except K which was extracted from KH (Alfa Aesar, 35% in mineral oil). The mixture of 1.2 g was sealed in a niobium capsule of 5 mm in diameter and, then, introduced inside a cylindrical graphite heater. The chemical reaction occurred under 3.5 GPa for 1 h at 800 °C; then, the sample was quenched and the pressure was released. The skutterudite phase formation was confirmed by laboratory X-ray diffraction (Cu-Kα radiation; λ = 1.54053 Å). Details on the synthesis and room condition structural properties of HP-synthesized $M_{0.5}Co_4Sb_{12}$ can be found elsewhere.[11−14,20]

2.2. High-Pressure Characterization. High-pressure investigations were performed in powder samples on the high-pressure/microdiffraction station of the BL04-MSPD beamline[21] of the CELLS-ALBA synchrotron (Barcelona, Spain), selecting an incident beam at Cd *K*-edge (λ = 0.4642 Å). Two diamond anvil cells with diamond culet sizes ranging from 500 to 700 μm were used; the pressure chambers were 200 and 300 μm hole drilled in a 50 μm-thick pre-indented Inconel gasket. Silicone oil was used as pressure transmitting medium: "Rhodorsil 47V1000" commercialized by VCR.[22] Grains of copper were placed inside the pressure cavity and used as the pressure sensor through copper EOS.[23] The two-dimensional X-ray patterns were recorded using a Rayonix CCD detector. The sample−detector distance (180 mm) and the beam center position were calibrated from LaB_6 diffraction data measured under exactly the same conditions as the sample. The Debye−Scherrer rings formed were integrated using the DIOPTAS software.[24] The as-obtained patterns were refined by the Rietveld method in the framework of FULLPROF suite.[25] The following parameters were refined: zero-point error, background coefficients, scale factor, asymmetry correction factors, lattice parameters, atomic coordinates, and isotropic displacements.

2.3. Computational Details. The theoretical models were performed according to density functional theory (DFT) with PBE functional,[26] implemented in the CRYSTAL17 package.[27] The cobalt, antimonium, and potassium atomic centers were defined by the POB-TZVP basis set developed by Bredow and co-workers.[28−30] Lanthanides, potassium, and strontium atomic centers were defined by the effective core potential basis set developed by Maier and co-workers.[31]

The Coulomb and exchange series were controlled by a set of five thresholds (10^{-8}, 10^{-8}, 10^{-8}, 10^{-8}, and 10^{-16}), which represent the overlap and penetration for Coulomb integrals, the overlap for HF exchange integrals, and the pseudo-overlap, respectively. The used shirking factors were 6 and 6 for Pack−Monkhorst and Gilat net, respectively. The structure optimization convergence was achieved on gradient components and nuclear displacements with tolerances on their root mean square set to 0.0003 and 0.0012 a.u., respectively.

The bonds of the different models were analyzed by "Quantum Theory: Atoms in Molecules" (QTAIM), which provides a quantum description of the electron's characteristics in the chemical bonds. The QTAIM analysis was carried out with the TOPOND program within the CRYSTAL17 package.[32] The crystalline models were represented by VESTA software.

3. RESULTS AND DISCUSSION

High-pressure synchrotron X-ray diffraction measurements were carried out up to ∼12 GPa for the skutterudite compounds with the following nominal compositions: $\square Co_4Sb_{12}$, $K_{0.5}Co_4Sb_{12}$, $Sr_{0.5}Co_4Sb_{12}$, $La_{0.5}Co_4Sb_{12}$, $Ce_{0.5}Co_4Sb_{12}$, and $Yb_{0.5}Co_4Sb_{12}$. Figure 1 shows the near

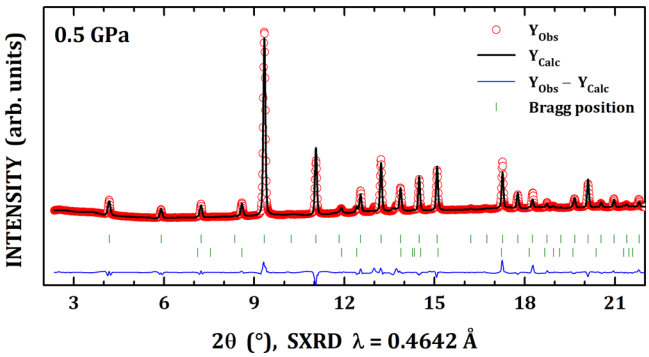

Figure 1. Near room condition synchrotron X-ray diffraction pattern of $\square Co_4Sb_{12}$ skutterudite. The second series of Bragg positions corresponds to Sb metal minor impurity.

room condition X-ray diffraction pattern of $\square Co_4Sb_{12}$, as refined according to the body-centered space group $Im\bar{3}$ ($N°$ 204, T_h^5) with eight formula per unit cell (Z = 8). The atomic distribution in this structure is the following: Co atoms are at 8*c* Wyckoff sites ($^1/_4$, $^1/_4$, $^1/_4$) and the Sb ones are positioned at 24*g* sites (0, *y*, *z*). Indeed, the *y* and *z* fractional coordinates and the lattice constant *a* are the only three parameters for representing the skutterudite crystal structure.[33] As depicted in Figure 2a, the skutterudite consists of a network of strongly tilted $[CoSb_6]$ octahedra sharing corners, forming large cages centered at 2*a* positions (0, 0, 0). These voids, represented by $\square$, may be filled by guest atoms. For pristine $\square Co_4Sb_{12}$, a minor impurity of Sb metal in a fraction of 6.1% was found after the refinement of the scale factors of both phases.

Under high-pressure conditions up to 12 GPa, the $\square Co_4Sb_{12}$ system did not exhibit any signal of structural phase transition, for instance, see the Rietveld refined pattern under 7.0 GPa in Figure 3a. Some details on the pressure

https://doi.org/10.1021/acs.inorgchem.1c00682
Inorg. Chem. 2021, 60, 7413−7421

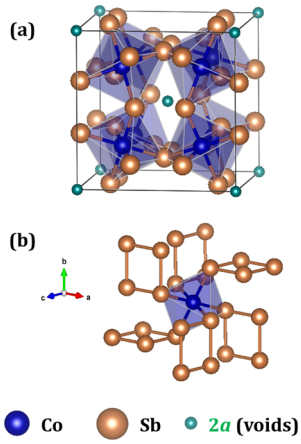

Figure 2. Sketch of the crystal structure of the filled skutterudite with guest atoms at 2*a* Wyckoff positions (a). View of the configuration of $[Sb_4]$ rings that exist in such a structure (b).

evolution of the secondary minor impurity of Sb metal are shown in Figure 3b. In particular, the Sb metal has a rhombohedral unit cell (S.G. $R\bar{3}m$) under room conditions, which undergoes two successive transitions to cubic (7.0 GPa) and hexagonal (8.5 GPa) phases.[34] However, in this work, only the hexagonal phase was identified under high pressure and starting at 9.4 GPa. In Figure 3c, the room-condition Sb rhombohedral phase was replaced by the close-packed hexagonal structure (S.G. $P6_3/mmc$) in order to refine the synchrotron X-ray pattern under 11.9 GPa. It is clear that the transition takes place at 9.4 GPa and the hexagonal phase is completely stabilized at 10.1 GPa.

Although previous works in the literature already reported the isothermal equation of state for pure $\square Co_4Sb_{12}$, we also performed here a high-pressure study of this compound. In our case, the skutterudites were fabricated using HP synthesis at moderate temperatures. Therefore, it would be interesting to probe their structural behavior under high pressure. The main reason for that is the improved thermoelectric properties observed in HP-synthesized skutterudites in recent years.[11−14] For example, the total thermal conductivity (κ_T) at room temperature in $\square Co_4Sb_{12}$ synthesized by conventional methods reaches values of 10 Wm^{-1} K^{-1}, while those HP-prepared depict a κ_T of 4.3 Wm^{-1} K^{-1},[20] based on the structural defects. It means that the HP condition has a pivotal role in enhancing the thermoelectric behavior in skutterudites.

Figure 4a represents the evolution of the relative volume (V/V_0) as a function of pressure for $\square Co_4Sb_{12}$ within the interval from 0.5 up to 11.9 GPa. V_0 stands for the unit-cell volume under atmospheric conditions, which was already known for each compound before the HP experiment (see in Table 1). One may notice that no discontinuity was detected in the unit-cell volume in such a pressure regime, which is the quasi-hydrostatic regime for silicone oil used here.[22] The experimental data were adjusted to the third-order Birch−Murnaghan (BM) isothermal equation of state (EOS)[35] as follows:

$$P(V) = \frac{3}{2}B_0\left[\left(\frac{V}{V_0}\right)^{-7/3} - \left(\frac{V}{V_0}\right)^{-5/3}\right]\left\{1 + \frac{3}{4}(B_0' - 4)\left[\left(\frac{V}{V_0}\right)^{-2/3} - 1\right]\right\} \quad (1)$$

which allows us to determine the Bulk modulus (B_0) and its pressure derivative ($B_0' = \partial B_0/\partial P$). In particular, the B_0' parameter was kept equal to 4. Table 1 summarizes the B_0 value for $\square Co_4Sb_{12}$ obtained from this work. The interesting result is that our $\square Co_4Sb_{12}$ has a B_0 of 100.4(3) GPa, which means that the HP synthesis makes the skutterudite more resistant to the compression when compared to the cobalt antimony prepared by conventional methods (B_0 = 93.2(6)[36]).

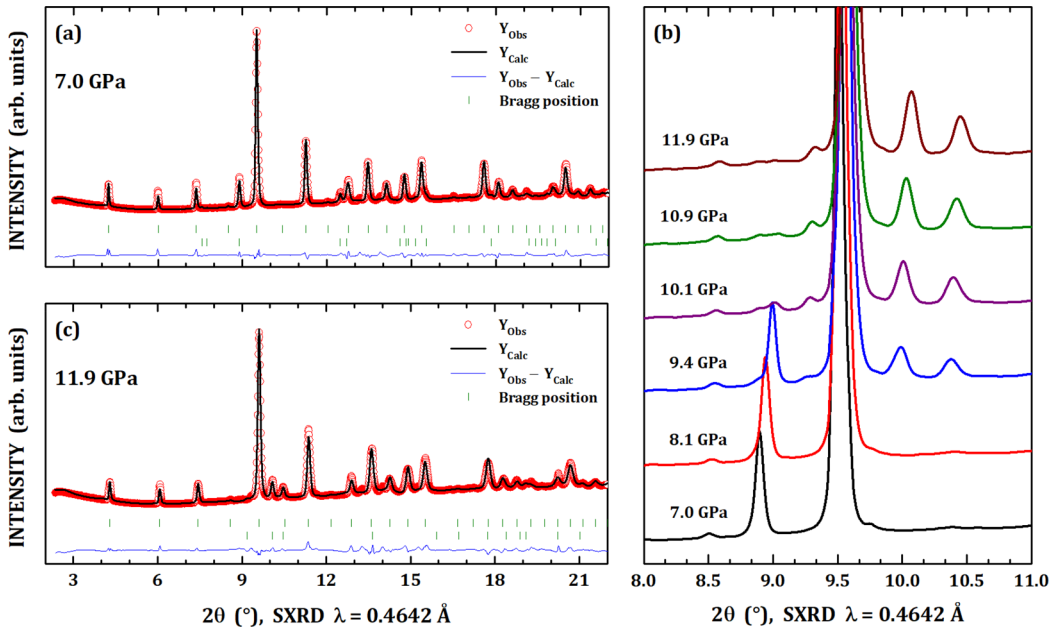

Figure 3. Synchrotron X-ray diffraction patterns of $\square Co_4Sb_{12}$ under 7.0 GPa (a) and 11.9 GPa (c). Details on the pressure evolution of Sb metal secondary phase (b), showing its phase transition from a rhombohedral (S.G. $R\bar{3}m$) to close-packed hexagonal (S.G. $P6_3/mmc$) phase around 9.4 GPa.

https://doi.org/10.1021/acs.inorgchem.1c00682
Inorg. Chem. 2021, 60, 7413−7421

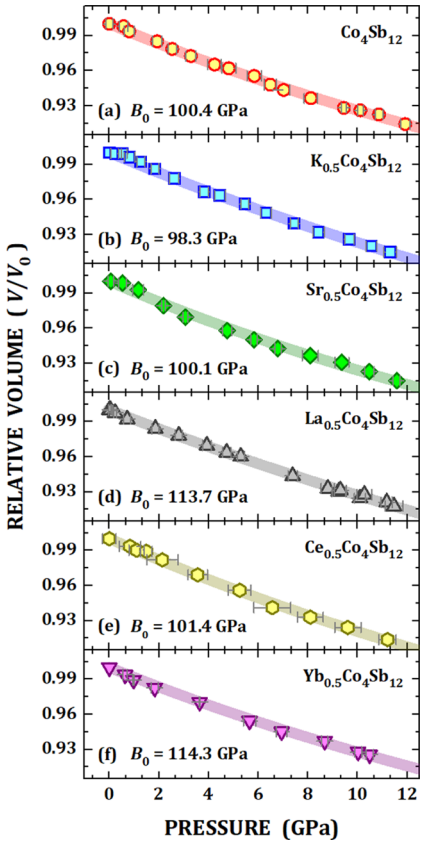

Figure 4. Relative volume (V/V_0) as a function of applied pressure (open symbols) together with the third-order Birch−Murnaghan (BM) equation of state (EOS) fitting (thick lines). The fitting was performed for the unfilled $\square Co_4Sb_{12}$ (a) and filled $M_{0.5}Co_4Sb_{12}$ skutterudites, in which M = K (b), Sr (c), La (d), Ce (e), and Yb (f).

Also, it is even more resistant than the $\square Co_4Sb_{12}$ prepared using a wedge-type cubic-anvil high-pressure apparatus (B_0 = 81(1) GPa[37]).

As pointed out earlier, the skutterudite structure can be viewed as eight subcubes cornered by Co atoms, with planar [Sb_4] rectangles occupying six of these cubes (Figure 2b) and, then, leaving two void spaces for a guest atom (at 2*a* sites) (see in Figure 2a). Such a filler atom may affect the local bonding of [Sb_4] units of Figure 2b and, therefore, the electronic band structure near the Fermi level.[33] The amount *f* of guest atoms into the voids is usually limited by the filling fraction limit, which depends on the chemical nature of the fillers (such as its electronegativity[38]) and their cationic sizes. In the single-filled skutterudite $M_fCo_4Sb_{12}$, the value of *f* barely reaches 0.25 for rare-earth elements (except for Eu with *f* = 0.45); for alkali and alkaline-earth metals, the filling fraction limit reaches *f* = 0.45 for K and 0.40 for Sr.[39] In our previous works, we reported on the high-pressure synthesis and structural characterization of filled $M_{0.5}Co_4Sb_{12}$ skutterudites;[11−14] two conclusions were obtained: the HP condition followed by quenching leads to two coexisting filled phases with uneven filling fractions, and this coexistence contributes to the reduced thermal conductivity. Probably, the inhomogeneous distribution of pressure within the Nb capsule, in intergranular regions with respect to the bulk of the grains, leads to the mentioned filling fraction distribution. The reduction of the thermal conductivity is achieved by creating a new hierarchy at the nanoscale. In this way, the HP-synthesized skutterudites present an all-length-scale hierarchy atomic scale with fillers, nanoscale with coexisting phases, and mesoscale with grain boundary effects. This hierarchy enhances the phonon scattering, thus decreasing the thermal conductivity at a macroscopic level.

The coexisting phases were detected due to the splitting of synchrotron X-ray diffraction peaks at high scattering angles, being collected in high-angular resolution mode.[21] For the diffraction experiments in high-pressure mode, the information

Table 1. Lattice Constants under Room Conditions (a) and Bulk Modulus (B_0) for Unfilled $\square Co_4Sb_{12}$ and Filled $M_{0.5}Co_4Sb_{12}$ (M = K, Sr, La, Ce, and Yb) Skutterudites

	this work				SXRD in refs11−14	
	2D detector		DFT		high angular resolution mode	
composition	a (Å)	B_0 (GPa)	a (Å)	B_0 (GPa)	a (Å)	
$\square Co_4Sb_{12}$	9.0358(8)	100.4	9.083	93.8	$\square Co_4Sb_{11.6}$ 9.03588(2)	
$K_{0.5}Co_4Sb_{12}$	9.0559(3)	98.3	9.149	88.8	$K_{0.13}Co_4Sb_{12}$ 9.0459(1)	$K_{0.11}Co_4Sb_{12}$ 9.03917(8)
$Sr_{0.5}Co_4Sb_{12}$	9.0887(5)	100.1	9.139	92.9	$Sr_{0.48}Co_4Sb_{12}$ 9.0887(7)	Co_4Sb_{12} 9.0393(7)
$La_{0.5}Co_4Sb_{12}$	9.0508(5)	113.7	9.123	94.6	$La_{0.17}Co_4Sb_{11.64}$ 9.0545(8)	$La_{0.052}Co_4Sb_{11.68}$ 9.0405(8)
$Ce_{0.5}Co_4Sb_{12}$	9.0480(5)	101.4	9.130	91.4	$Ce_{0.10}Co_4Sb_{11.64}$ 9.04805(5)	$Ce_{0.05}Co_4Sb_{11.64}$ 9.03940(6)
$Yb_{0.5}Co_4Sb_{12}$	9.0512(5)	114.3			$Yb_{0.26}Co_4Sb_{11.54}$ 9.06186(4)	$Yb_{0.06}Co_4Sb_{11.54}$ 9.0444(1)

https://doi.org/10.1021/acs.inorgchem.1c00682
Inorg. Chem. 2021, 60, 7413−7421

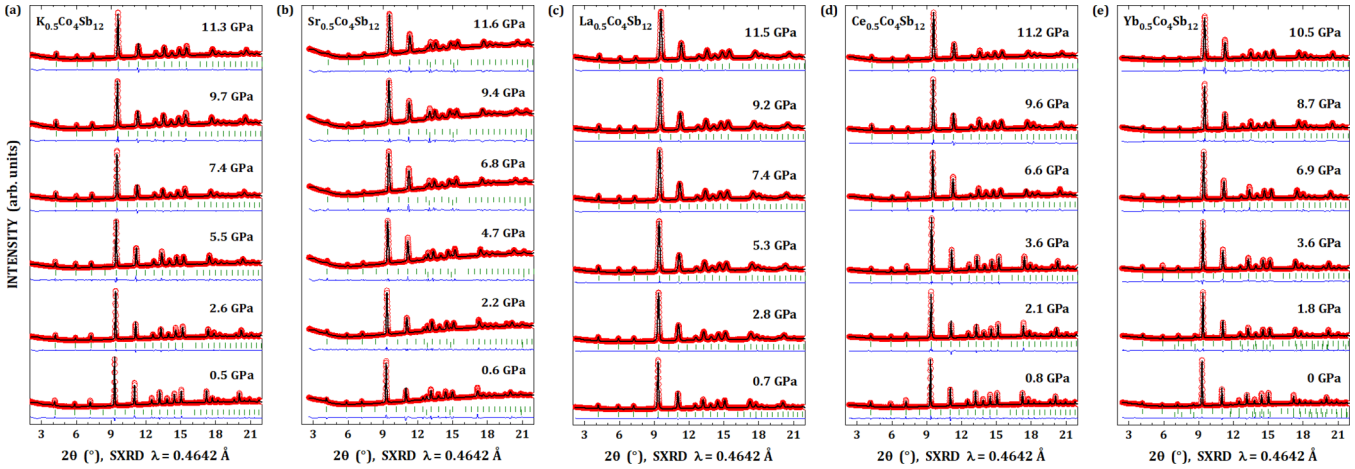

Figure 5. Synchrotron X-ray diffraction patterns of the filled $M_{0.5}Co_4Sb_{12}$ skutterudites under selected pressures, in which M = K (a), Sr (b), La (c), Ce (d), and Yb (e). Red open circles represent the experimental data, the black line refers to the calculated profile, the blue line is the difference between experimental and calculated data, and dark green bars denote the Bragg reflections.

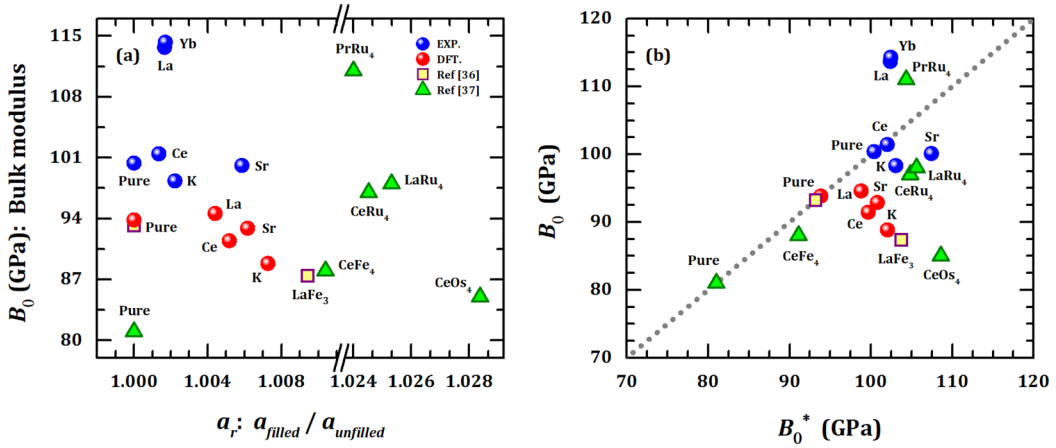

Figure 6. (a) Bulk modulus (B_0) against the relative lattice constant a_r (a_r = $a_{filled}/a_{unfilled}$) for the unfilled Co_4Sb_{12} (denoted as "pure") and $M_{0.5}Co_4Sb_{12}$ skutterudites (M = K, Sr, La, Ce, and Yb) investigated. It also includes the B_0 values for filled skutterudites MRu_4Sb_{12} (M = La and Pr), CeT_4Sb_{12} (T = Fe, Ru, and Os),[37] and $LaFe_3CoSb_{12}$.[36] (b) Comparison between Bulk modulus calculated from eq 2 (B_0*) and theoretically/experimentally obtained (B_0). The gray dotted line stands for B_0 = B_0*.

on the coexisting phases was lost since there is one order of magnitude difference of angular resolution between the two modes. As a result, the peak splitting was not indeed detected, and the refinement only gives one single skutterudite phase for all the filled samples. On the other hand, the effect of filling could be detected by the lattice expansion (see in Table 1), which shows that the filler element entered into the skutterudite structure. Despite some differences, we concluded that the lattice constants collected under high pressure would, at least, represent the filled skutterudite phase with the greatest filling fraction reached for each filled $M_{0.5}Co_4Sb_{12}$.

From a crystallo-chemical point of view, the guest atom tends to expand the unit-cell volume, depending on the filling fraction, and it would decrease the compressibility of filled skutterudites. In the literature, the opposite behavior was observed by Kraemer *et al.*[36] for $LaFe_3CoSb_{12}$ (B_0 = 87.4(6) GPa) in comparison with the unfilled $\square Co_4Sb_{12}$ (B_0 = 93.2(6) GPa). However, such a compound has the effect of both Fe and Co atoms in the doped filled skutterudite structure. In our case, we aim to evaluate only the effect of chemical pressure generated by the guest atoms at 2*a* positions in binary $\square Co_4Sb_{12}$. In this way, synchrotron X-ray diffraction studies under high pressure (0 up to 12 GPa) were performed in the following filled $M_{0.5}Co_4Sb_{12}$ skutterudites, for M = K, Sr, La, Ce, and Yb. Different valence states 1+ (K), 2+ (Sr), and 3+ (La, Ce, and Yb) were chosen in order to provide more information on the charge transfer and its role in compressibility of filled skutterudites.

Figure 5 shows some refined patterns under selected pressures for each filler element, i.e., K (a), Sr (b), La (c), Ce (d), and Yb (e). No new peaks are observed in the diffraction patterns, although the reflection lines shift to high angle with increasing pressure, as expected. A good quality refinement was obtained for all the compounds in all the range of investigated pressures. The samples with K, La, and Ce atoms were refined using only a single skutterudite phase with the filler element at the 2*a* position, while for Sr and Yb, a second phase of Cu and Sb metals was introduced in the refinement, respectively. For all the samples, the Cu metal is a pressure sensor. Panels (b) to (f) of Figure 4 depict the evolution of the relative volume (V/V_0) as a function of pressure up to 12 GPa for the filled skutterudites investigated in this work. The fitting by the third-order Birch−Murnaghan (BM) isothermal equation of state (EOS) revealed some

https://doi.org/10.1021/acs.inorgchem.1c00682
Inorg. Chem. 2021, 60, 7413−7421

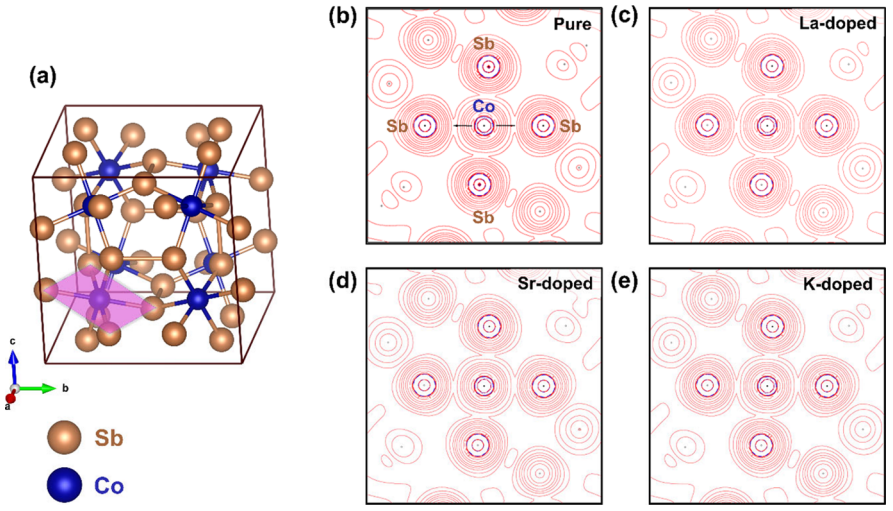

Figure 7. 3D structure highlighting the plane of interest for topochemical studies (pink) (a). Laplacian of electronic density isolines of the Co−Sb interaction (b−e).

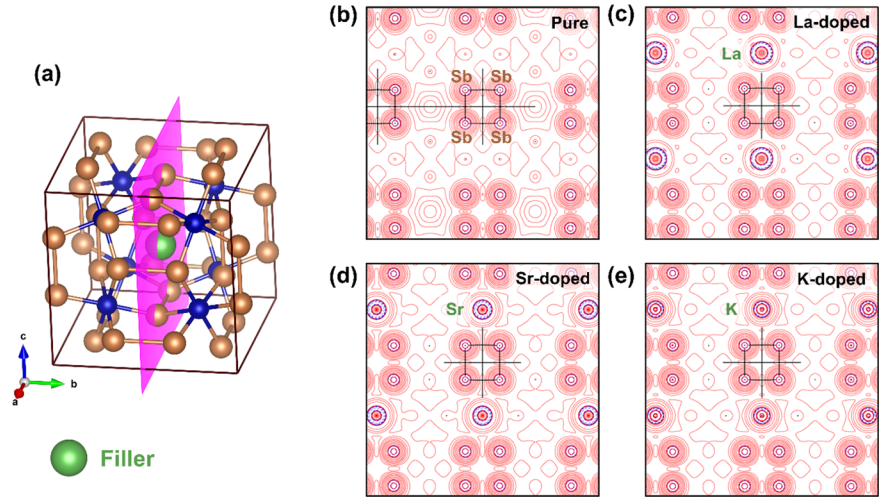

Figure 8. 3D structure highlighting the plane of interest for topochemical studies (pink) (a). Laplacian of electronic density isolines of the M−Sb and Sb−Sb interactions (b−e). The [Sb_4] ring is represented in each plane.

changes in the Bulk modulus, as compared to the unfilled □Co_4Sb_{12} (see in Table 1).

Theoretical models according to the DFT method were used to better understand the high-pressure behavior in the filled skutterudites. A filling fraction limit of $f = 0.5$ was considered for all the simulated filled samples: K, Sr, La, and Ce. The effect of hydrostatic pressure was simulated in unfilled □Co_4Sb_{12} and filled compounds ranging from ∼0 up to 12 GPa. The lattice constants optimized for the calculations are shown in Table 1. Although perfect agreement was not reached, one may see the filler effect by expanding the lattice constant. The calculated relative volume (V/V_0) as a function of pressure for each referred sample is displayed in Figure 4. Table 1 also includes the Bulk modulus from DFT calculations for the referred filled skutterudites investigated in this work.

A better comparison between experimental and calculated Bulk modulus is shown in Figure 6a, in which this parameter is plotted against the relative lattice constant a_r ($a_r = a_{filled}/a_{unfilled}$), being defined as the ratio between lattice constant of filled skutterudite and that for the unfilled sample. Also plotted in Figure 6a are the Bulk moduli for filled skutterudites MRu_4Sb_{12} (M = La and Pr), CeT_4Sb_{12} (T = Fe, Ru, and Os),[37] and $LaFe_3CoSb_{12}$.[36] Except for $K_{0.5}Co_4Sb_{12}$ and $LaFe_3CoSb_{12}$, the lattice expansion, at least, leads to an increase in the Bulk modulus. When K is the filler atom, the general tendency observed for both experimental and theoretical techniques is to reduce B_0 and, therefore, to enhance the compressibility. The Bulk modulus is almost unchanged for the K filling. Significant variations in the B_0 value were observed for La and Yb (B_0 ∼ 114 GPa) as fillers in □Co_4Sb_{12} (B_0 ∼ 100 GPa). It is also worth mentioning that the La- and Yb-filled samples depict the highest values of B_0 among the antimony-based skutterudites in Figure 6.

Topochemical analysis of the bond order of the filler site environment was carried out to evaluate the atomic bond variations between the different systems. Figures 7 and 8 exhibit the planes and bonds that have been considered. Table 2 presents the density, Laplacian electron density, bond degree, and $|V|/G$ ratio.

Starting the data evaluation of the pure □Co_4Sb_{12} system, it was noted that, in a general observation, it presents transient bonds with a tendency leaning slightly toward the ionic character. This can be seen by the low $\rho(r)$ values and positive values of $\nabla^2\rho(r)$. As expected, the Sb−Sb interaction presents

https://doi.org/10.1021/acs.inorgchem.1c00682
Inorg. Chem. 2021, 60, 7413−7421

Table 2. Topochemical Parameters of Pure and Doped □Co_4Sb_{12} Crystals at the Bond Critical Point: Charge Density ($\rho(r)$), Laplacian of Electron Density ($\nabla^2\rho(r)$), $|V|/G$ ratio, and Bond Degree ($H/\rho(r)$)[a]

composition	bond	ρ	$\nabla^2\rho$	$\lvert V\rvert/G$	H/ρ
□Co_4Sb_{12}	Co−Sb	0.060	0.066	1.501	−0.275
	Sb−Sb	0.044	0.007	1.833	−0.209
	Sb−Sb	0.052	0.005	1.907	−0.248
$K_{0.5}Co_4Sb_{12}$	Co−Sb	0.058	0.065	1.484	−0.264
	Sb−Sb	0.042	0.010	1.780	−0.199
	Sb−Sb	0.050	0.007	1.864	−0.238
	K−Sb	0.010	0.031	0.832	0.109
$Sr_{0.5}Co_4Sb_{12}$	Co−Sb	0.058	0.064	1.488	−0.264
	Sb−Sb	0.043	0.008	1.809	−0.203
	Sb−Sb	0.050	0.006	1.884	−0.241
	Sr−Sb	0.012	0.037	0.913	0.060
$La_{0.5}Co_4Sb_{12}$	Co−Sb	0.058	0.064	1.485	−0.263
	Sb−Sb	0.043	0.008	1.807	−0.203
	Sb−Sb	0.050	0.007	1.876	−0.238
	La−Sb	0.020	0.035	1.125	−0.061

[a]V: virial potential energy, G: kinetic energy density, and H: total energy density.

$\nabla^2\rho(r)$ smaller and $|V|/G$ close to 2, which means a less ionic character as compared to Co−Sb bonds.[40]

With the addition of the fillers, in all models, a slight decrease in the values of $\rho(r)$ and an increase in $\nabla^2\rho(r)$ of the Co−Sb and Sb−Sb connections are observed. Our simulation used M = K, Sr, and La as representative situations for the next valence states 1+, 2+, and 3+, respectively. This fact represents a slight disturbance and an increase, even if it is small, in the ionic character of the system as a whole. In addition, another interesting factor is the M−Sb interaction around the filler site. For Sr and K fillers, values of 0.012 and 0.010 of $\rho(r)$ and 0.037 and 0.031 of $\nabla^2\rho(r)$ show less localized electrons between the M−Sb nuclei in relation to the Co−Sb bonds. In addition, values lower than 1 of $|V|/G$ and the inversion of the H/ρ magnitude (positive) indicate "closed-shell" bonds with ionic/van der Walls interactions. On the other hand, values of $|V|/G$ greater than 1 and H/ρ negative observed in La−Sb indicate an interaction with a covalent incipient character. The H/ρ negative also indicates a higher direct bond interaction between the La and the Sb site neighbors. This fact shows that La incorporates different interactions than those incorporated by Sr and K.

The presence of the filler inside the voids generates an internal pressure, which is responsible for the lattice expansion observed under ambient conditions. Then, the Bulk modulus of the expanded structure (B_0*), as compared to the unfilled □Co_4Sb_{12} ($B_{0|un}$), would be approached by $B_0^* - B_{0|un} \approx B_0'\Delta P$. The variation in pressure ΔP can be replaced by $-B_{0|un}\Delta V/V_{0|un}$, in view of the Bulk modulus definition; ΔV represents the volume expansion induced by the filler. Different from the assumption taken by Kraemer *et al.*,[36] we have considered that ΔP has a negative sign since the direction of the pressure field inside the voids is opposite to that in typical experiments of compression:

$$B_0^* \approx B_{0|un}\left(1 + B_0'\frac{\Delta V}{V_{0|un}}\right) \quad (2)$$

In Figure 6b, a comparison between the Bulk modulus as evaluated by eq 2 and those experimentally/theoretically obtained is shown. One may see that a poor agreement is achieved, which means that a simple lattice expansion is not enough to account for the variation of the Bulk modulus in filled skutterudites.

It is clear that a more complex interaction among the fillers and the skutterudite framework takes place in filled skutterudites, which is not accounted by eq 2. An electronic model for this behavior considers that the filler M donates their valence electrons to the conduction band of the skutterudite framework and, therefore, the character of the chemical bonds between the filler and the Sb framework atoms has an ionic character. Such a fact can be observed by the variation in the electronic charge around the [Sb_4] ring when the fillers enter into the skutterudite structure (see in Table 2). Then, the variation in the Bulk modulus in the presence of the filler elements not only has a component coming from the volume expansion, but the charge localization and ionic character of the filled samples will also contribute to the Bulk modulus changes.

Recently, Hanus *et al.*[33] studied the local thermal expansion of Co−Sb and Sb−Sb bonds within Yb-filled Co_4Sb_{12} skutterudite by synchrotron X-ray diffraction. They established, from computational results, the crucial role of the [Sb_4] ring local structure in predicting the electronic structure changes by means of band convergence. Wang *et al.*[41] concluded that the filler acts on the A_g phonon mode of the [Sb_4] ring by stretching and compression of the vibration, which affects the Sb−Sb antibonding states. Those states are crucial for the valence band maximum, and therefore, the band gap becomes tunable. In our case, we have observed for K-, Sr-, and La-filled Co_4Sb_{12} skutterudites that the filler induces a disturbance and an increased ionic character within the lattice. As a result, the high-pressure behavior presented slight changes by means of the Bulk modulus. High-pressure studies are shown to be a promising method to probe the filler effects in skutterudites for thermoelectric applications.

4. CONCLUSIONS

In this work, we investigated the high-pressure behavior of unfilled □Co_4Sb_{12} and filled $M_{0.5}Co_4Sb_{12}$ (M = K, Sr, La, Ce, and Yb) skutterudites by synchrotron X-ray diffraction. The skutterudite compounds were also synthesized under high pressure, as we reported previously in refs 11−14. In the pressure range 0−12 GPa, the EOS were obtained and the Bulk moduli (B_0) were estimated for all the filled skutterudites. The Bulk modulus of each composition was estimated and compared to the values calculated by DFT methods. We also estimated the variation of B_0 using a linear approach to predict its values (see in eq 2). We concluded that a simple lattice expansion due to the filler atoms is not enough to describe the experimentally derived B_0 values. Topochemical investigations of the filler site environment were carried out in order to evaluate the bond changes as a function of the filler element. The theoretical results showed a slight disturbance and an increased ionic character when the filler is stabilized inside the skutterudite voids, and therefore, the mechanical properties are indeed affected, as we observed in the Bulk modulus.

https://doi.org/10.1021/acs.inorgchem.1c00682
Inorg. Chem. 2021, 60, 7413−7421

AUTHOR INFORMATION

Corresponding Authors

João Elias F. S. Rodrigues − *Instituto de Ciencia de Materiales de Madrid, CSIC, E-28049 Madrid, Spain; European Synchrotron Radiation Facility, ESRF, 38000 Grenoble, France;* orcid.org/0000-0002-9220-5809; Email: rodrigues.joaoelias@esrf.fr, rodrigues.joaoelias@gmail.com

José A. Alonso − *Instituto de Ciencia de Materiales de Madrid, CSIC, E-28049 Madrid, Spain;* orcid.org/0000-0001-5329-1225; Email: ja.alonso@icmm.csic.es

Authors

Javier Gainza − *Instituto de Ciencia de Materiales de Madrid, CSIC, E-28049 Madrid, Spain;* orcid.org/0000-0002-1999-3116

Federico Serrano-Sánchez − *Instituto de Ciencia de Materiales de Madrid, CSIC, E-28049 Madrid, Spain*

Mateus M. Ferrer − *CCAF, PPGCEM/CDTec, Federal University of Pelotas, 96010-610 Pelotas, Rio Grande do Sul, Brazil*

Guilherme S. L. Fabris − *Materials Science and Engineering Postgraduate Program, Department of Materials Engineering, Federal University of Rio Grande do Norte, 59078-970 Natal, Brazil;* orcid.org/0000-0002-0830-5787

Julio R. Sambrano − *Modeling and Molecular Simulation Group, São Paulo State University, 17030-360 Bauru, SP, Brazil;* orcid.org/0000-0002-5217-7145

Norbert M. Nemes − *Departamento de Física de Materiales, Universidad Complutense de Madrid, E-28040 Madrid, Spain*

José L. Martínez − *Instituto de Ciencia de Materiales de Madrid, CSIC, E-28049 Madrid, Spain*

Catalin Popescu − *CELLS−ALBA Synchrotron, E-08290 Cerdanyola del Valles, Barcelona, Spain*

Complete contact information is available at: https://pubs.acs.org/10.1021/acs.inorgchem.1c00682

Notes

The authors declare no competing financial interest.

ACKNOWLEDGMENTS

The Spanish authors thank the Spanish Ministry of Science, Innovation, and Universities for funding the project number: MAT2017-84496-R. J.G. thanks MICINN for granting the contract: PRE2018-083398. C.P. acknowledges the financial support from the Spanish Ministry of Economy and Competitivity through the FIS2017-83295-P project. M.F. and J.R. thank the Brazilian funding agency CNPq through the project: 432242/2018-0. J.S. thanks the Brazilian funding agency FAPESP through the project: 2019/08928-9. G.F. thanks the Brazilian funding agency CAPES through the project 88887.467334/2019-00 (Finance Code 001). The authors wish to express their gratitude to CELLS-ALBA technical staff for making the facilities available for the synchrotron X-ray powder diffraction experiments number: 2019023343.

REFERENCES

(1) Snyder, G. J.; Toberer, E. S. Complex Thermoelectric Materials. *Nat. Mater.* **2008**, *7*, 105−114.

(2) Slack, G. A. New Materials and Performance Limits for Thermoelectric Cooling. In *CRC Handbook of Thermoelectrics*; Rowe, D. M., Ed.; CRC Press: Boca Raton, FL, 1995; pp. 407−440.

(3) Nolas, G. S.; Sharp, J.; Goldsmid, H. J. The Phonon—Glass Electron-Crystal Approach to Thermoelectric Materials Research. In *Thermoelectrics*; Springer: Berlin, Heidelberg, 2001; pp 177−207, DOI: 10.1007/978-3-662-04569-5_6.

(4) Tang, Y.; Hanus, R.; Chen, S. W.; Snyder, G. J. Solubility Design Leading to High Figure of Merit in Low-Cost Ce-$CoSb_3$ Skutterudites. *Nat. Commun.* **2015**, *6*, 1−7.

(5) Li, W.; Wang, J.; Xie, Y.; Gray, J. L.; Heremans, J. J.; Kang, H. B.; Poudel, B.; Huxtable, S. T.; Priya, S. Enhanced Thermoelectric Performance of Yb-Single-Filled Skutterudite by Ultralow Thermal Conductivity. *Chem. Mater.* **2019**, *31*, 862−872.

(6) Tang, Y.; Chen, S. w.; Snyder, G. J. Temperature Dependent Solubility of Yb in Yb−CoSb3 Skutterudite and Its Effect on Preparation, Optimization and Lifetime of Thermoelectrics. *J. Mater.* **2015**, *1*, 75−84.

(7) Said, S. M.; Bashir, M. B. A.; Sabri, M. F. M.; Miyazaki, Y.; Shnawah, D. A. A.; Hakeem, A. S.; Shimada, M.; Bakare, A. I.; Ghazali, N. N. N.; Elsheikh, M. H. Enhancement of Thermoelectric Behavior of $La_{0.5}Co_4Sb_{12-x}Te_x$ Skutterudite Materials. *Metall. Mater. Trans. A* **2017**, *48*, 3073−3081.

(8) Ali Bashir, M. B.; Mohd Said, S.; Mohd Sabri, M. F.; Miyazaki, Y.; Ameer Shnawah, D. A.; Shimada, M.; Elsheikh, M. H. Enhancement of Thermoelectric Properties of $Yb_{0.25}Co_4Sb_{12}$ Skutterudites through Ni Substitution. *Sains Malays.* **2018**, *47*, 181−187.

(9) Li, H.; Tang, X.; Zhang, Q.; Uher, C. High Performance $In_xCe_yCo_4Sb_{12}$ thermoelectric Materials with in Situ Forming Nanostructured InSb Phase. *Appl. Phys. Lett.* **2009**, *94*, 102114.

(10) Mi, J.-L.; Christensen, M.; Nishibori, E.; Iversen, B. B. Multitemperature Crystal Structures and Physical Properties of the Partially Filled Thermoelectric Skutterudites $M_{0.1}Co_4Sb_{12}$ (M = La, Ce, Nd, Sm, Yb and Eu). *Phys. Rev. B* **2011**, *84*, 064114.

(11) Gainza, J.; Serrano-Sánchez, F.; Rodrigues, J. E.; Prado-Gonjal, J.; Nemes, N. M.; Biskup, N.; Dura, O. J.; Martínez, J. L.; Fauth, F.; Alonso, J. A. Unveiling the Correlation between the Crystalline Structure of M-Filled $CoSb_3$ (M = Y, K, Sr) Skutterudites and Their Thermoelectric Transport Properties. *Adv. Funct. Mater.* **2020**, *30*, 2001651.

(12) Serrano-Sánchez, F.; Prado-Gonjal, J.; Nemes, N. M.; Biskup, N.; Varela, M.; Dura, O. J.; Martínez, J. L.; Fernández-Díaz, M. T.; Fauth, F.; Alonso, J. A. Low Thermal Conductivity in La-Filled Cobalt Antimonide Skutterudites with an Inhomogeneous Filling Factor Prepared under High-Pressure Conditions. *J. Mater. Chem. A* **2018**, *6*, 118−126.

(13) Serrano-Sánchez, F.; Prado-Gonjal, J.; Nemes, N. M.; Biskup, N.; Dura, O. J.; Martínez, J. L.; Fernández-Díaz, M. T.; Fauth, F.; Alonso, J. A. Thermal Conductivity Reduction by Fluctuation of the Filling Fraction in Filled Cobalt Antimonide Skutterudite Thermoelectrics. *ACS Appl. Energy Mater.* **2018**, *1*, 6181−6189.

(14) Gainza, J.; Serrano-Sánchez, F.; Prado-Gonjal, J.; Nemes, N. M.; Biskup, N.; Dura, O. J.; Martínez, J. L.; Fauth, F.; Alonso, J. A. Substantial thermal conductivity reduction in mischmetal skutterudites $Mm_xCo_4Sb_{12}$ prepared under high-pressure conditions, due to uneven distribution of the rare-earth elements. *J. Mater. Chem. C* **2019**, *7*, 4124−4131.

(15) Miyake, A.; Shimizu, K.; Sekine, C.; Kihou, K.; Shirotani, I. Pressure-Induced Superconductivity in Filled Skutterudite $PrRu_4P_{12}$. *J. Phys. Soc. Jpn.* **2004**, *73*, 2370−2372.

(16) Takizawa, H.; Miura, K.; Ito, M.; Suzuki, T.; Endo, T. Atom Insertion into the $CoSb_3$ Skutterudite Host Lattice under High Pressure. *J. Alloys Compd.* **1999**, *282*, 79−83.

(17) Nolas, G. S.; Takizawa, H.; Endo, T.; Sellinschegg, H.; Johnson, D. C. Thermoelectric Properties of Sn-Filled Skutterudites. *Appl. Phys. Lett.* **2000**, *77*, 52−54.

(18) Yang, J.; Zhang, L.; Liu, Y.; Chen, C.; Li, J.; Yu, D.; He, J.; Liu, Z.; Tian, Y.; Xu, B. Investigation of Skutterudite $Mg_yCo_4Sb_{12}$: High

Pressure Synthesis and Thermoelectric Properties. *J. Appl. Phys.* **2013**, *113*, 113703.
(19) Kraemer, A. C.; Gallas, M. R.; da Jornada, J. A. H.; Perottoni, C. A. Pressure-Induced Self-Insertion Reaction in $CoSb_3$. *Phys. Rev. B* **2007**, *75*, 024105.
(20) Prado-Gonjal, J.; Serrano-Sánchez, F.; Nemes, N. M.; Dura, O. J.; Martínez, J. L.; Fernández-Díaz, M. T.; Fauth, F.; Alonso, J. A. Extra-Low Thermal Conductivity in Unfilled $CoSb_{3-\delta}$ Skutterudite Synthesized under High-Pressure Conditions. *Appl. Phys. Lett.* **2017**, *111*, 083902.
(21) Fauth, F.; Boer, R.; Gil-Ortiz, F.; Popescu, C.; Vallcorba, O.; Peral, I.; Fullà, D.; Benach, J.; Juanhuix, J. The Crystallography Stations at the Alba Synchrotron. *Eur. Phys. J. Plus* **2015**, *130*, 160.
(22) Klotz, S.; Chervin, J.-C.; Munsch, P.; Le Marchand, G. Hydrostatic Limits of 11 Pressure Transmitting Media. *J. Phys. D: Appl. Phys.* **2009**, *42*, No. 075413.
(23) Dewaele, A.; Loubeyre, P.; Mezouar, M. Equations of State of Six Metals above 94 GPa. *Phys. Rev. B* **2004**, *70*, 1−8.
(24) Prescher, C.; Prakapenka, V. B. DIOPTAS: A Program for Reduction of Two-Dimensional X-Ray Diffraction Data and Data Exploration. *High Pressure Res.* **2015**, *35*, 223−230.
(25) Rodríguez-Carvajal, J. Recent Advances in Magnetic Structure Determination by Neutron Powder Diffraction. *Phys. B: Condens. Matter* **1993**, *192*, 55−69.
(26) Perdew, J. P.; Burke, K.; Ernzerhof, M. Generalized Gradient Approximation Made Simple [Phys. Rev. Lett. 77, 3865 (1996)]. *Phys. Rev. Lett.* **1997**, *78*, 1396−1396.
(27) Dovesi, R.; Erba, A.; Orlando, R.; Zicovich-Wilson, C. M.; Civalleri, B.; Maschio, L.; Rérat, M.; Casassa, S.; Baima, J.; Salustro, S.; Kirtman, B. Quantum-Mechanical Condensed Matter Simulations with CRYSTAL. *Wiley Interdiscip. Rev.: Comput. Mol. Sci.* **2018**, *8*, No. e1360.
(28) Vilela Oliveira, D.; Laun, J.; Peintinger, M. F.; Bredow, T. BSSE-Correction Scheme for Consistent Gaussian Basis Sets of Double- and Triple-Zeta Valence with Polarization Quality for Solid-State Calculations. *J. Comput. Chem.* **2019**, *40*, 2364−2376.
(29) Laun, J.; Vilela Oliveira, D.; Bredow, T. Consistent Gaussian Basis Sets of Double- and Triple-Zeta Valence with Polarization Quality of the Fifth Period for Solid-State Calculations. *J. Comput. Chem.* **2018**, *39*, 1285−1290.
(30) Peintinger, M. F.; Oliveira, D. V.; Bredow, T. Consistent Gaussian Basis Sets of Triple-Zeta Valence with Polarization Quality for Solid-State Calculations. *J. Comput. Chem.* **2013**, *34*, 451−459.
(31) Heifets, E.; Kotomin, E. A.; Bagaturyants, A. A.; Maier, J. Ab Initio Study of $BiFeO_3$: Thermodynamic Stability Conditions. *J. Phys. Chem. Lett.* **2015**, *6*, 2847−2851.
(32) Casassa, S.; Erba, A.; Baima, J.; Orlando, R. Electron Density Analysis of Large (Molecular and Periodic) Systems: A Parallel Implementation. *J. Comput. Chem.* **2015**, *36*, 1940−1946.
(33) Hanus, R.; Guo, X.; Tang, Y.; Li, G.; Snyder, G. J.; Zeier, W. G. A Chemical Understanding of the Band Convergence in Thermoelectric $CoSb_3$ Skutterudites: Influence of Electron Population, Local Thermal Expansion, and Bonding Interactions. *Chem. Mater.* **2017**, *29*, 1156−1164.
(34) Vereshchagin, L. F.; Kabalkina, S. S. Phase Transitions in Antimony at High Pressures. *Sov. Phys. Jetp* **1965**, *20*, 274−277.
(35) Birch, F. Finite Elastic Strain of Cubic Crystals. *Phys. Rev.* **1947**, *71*, 809−824.
(36) Kraemer, A. C.; Perottoni, C. A.; Da Jornada, J. A. H. Isothermal Equation of State for the Skutterudites $CoSb_3$ and $LaFe_3CoSb_{12}$. *Solid State Commun.* **2005**, *133*, 173−176.
(37) Shirotani, I.; Noro, T.; Hayashi, J.; Sekine, C.; Giri, R.; Kikegawa, T. X-Ray Study with Synchrotron Radiation for P- and Sb-Based Skutterudite Compounds at High Pressures. *J. Phys.: Condens. Matter* **2004**, *16*, 7853−7862.
(38) Shi, X.; Zhang, W.; Chen, L. D.; Yang, J. Filling Fraction Limit for Intrinsic Voids in Crystals: Doping in Skutterudites. *Phys. Rev. Lett.* **2005**, *95*, 185503.
(39) Shi, X.; Bai, S.; Xi, L.; Yang, J.; Zhang, W.; Chen, L.; Yang, J. Realization of High Thermoelectric Performance in N-Type Partially Filled Skutterudites. *J. Mater. Res.* **2011**, *26*, 1745−1754.
(40) Kumar, P. S. V.; Raghavendra, V.; Subramanian, V. Bader's Theory of Atoms in Molecules (AIM) and Its Applications to Chemical Bonding. *J. Chem. Sci.* **2016**, *128*, 1527−1536.
(41) Wang, Z.; Xi, J.; Ning, J.; Guo, K.; Duan, B.; Luo, J.; Snyder, G. J.; Yang, J.; Zhang, W. Temperature-Dependent Band Renormalization in $CoSb_3$ Skutterudites Due to Sb-Ring-Related Vibrations. *Chem. Mater.* **2021**, *33*, 1046−1052.

https://doi.org/10.1021/acs.inorgchem.1c00682
Inorg. Chem. 2021, 60, 7413−7421